TECHNICAL REPORT ARBRL-TR-02323

PENETRATION WITH LONG RODS: A THEORETICAL FRAMEWORK AND COMPARISON WITH INSTRUMENTED IMPACTS

Thomas W. Wright

May 1981

US ARMY ARMAMENT RESEARCH AND DEVELOPMENT COMMAND
BALLISTIC RESEARCH LABORATORY
ABERDEEN PROVING GROUND, MARYLAND

Destroy this report when it is no longer needed.
Do not return it to the originator.

Secondary distribution of this report by originating or sponsoring activity is prohibited.

Additional copies of this report may be obtained from the National Technical Information Service, U.S. Department of Commerce, Springfield, Virginia 22161.

The findings in this report are not to be construed as an official Department of the Army position, unless so designated by other authorized documents.

The use of trade names or manufacturers' names in this report does not constitute indorsement of any commercial product.

REPORT DOCUMENTATION PAGE

READ INSTRUCTIONS BEFORE COMPLETING FORM

1. REPORT NUMBER: TECHNICAL REPORT ARBRL-TR-02323
2. GOVT ACCESSION NO.:
3. RECIPIENT'S CATALOG NUMBER:

4. TITLE (and Subtitle): Penetration with Long Rods: A Theoretical Framework and Comparison with Instrumented Impacts

5. TYPE OF REPORT & PERIOD COVERED: Final

6. PERFORMING ORG. REPORT NUMBER:

7. AUTHOR(s): Thomas W. Wright

8. CONTRACT OR GRANT NUMBER(s):

9. PERFORMING ORGANIZATION NAME AND ADDRESS
US Army Ballistic Research Laboratory
ATTN: DRDAR-BLT
Aberdeen Proving Ground, MD 21005

10. PROGRAM ELEMENT, PROJECT, TASK AREA & WORK UNIT NUMBERS: 1L161102AH43

11. CONTROLLING OFFICE NAME AND ADDRESS
US Army Armament Research and Development Command
US Army Ballistic Research Laboratory (DRDAR-BL)
Aberdeen Proving Ground, MD 21005

12. REPORT DATE: MAY 1981

13. NUMBER OF PAGES: 32

14. MONITORING AGENCY NAME & ADDRESS (if different from Controlling Office):

15. SECURITY CLASS. (of this report): UNCLASSIFIED

15a. DECLASSIFICATION/DOWNGRADING SCHEDULE:

16. DISTRIBUTION STATEMENT (of this Report)

Approved for public release; distribution unlimited.

17. DISTRIBUTION STATEMENT (of the abstract entered in Block 20, if different from Report)

18. SUPPLEMENTARY NOTES

19. KEY WORDS (Continue on reverse side if necessary and identify by block number)

penetration mechanics
long rods
eroding rod model
instrumented penetrator

20. ABSTRACT (Continue on reverse side if necessary and identify by block number) bet/2972

A critical review of the eroding rod model for deep penetration by long rods is presented. The chief difficulty lies in the use of the modified Bernoulli equation and of the over-simplified rigid-plastic material model, which is implied by that equation. It is concluded that even though the eroding rod model can give only limited insight into the details of the actual rod/target interaction, still it is useful in suggesting an experimental program to begin probing the details of the interaction process. The theoretical framework

underlying such a program is explained in detail. The theory of one dimensional wave propagation is used to show how data from instrumented long rods and targets may be fitted together to give a coherent picture of the time sequence of events during penetration. Data from one series of experiments, reported in detail elsewhere, is presented and discussed within the theoretical framework.

TABLE OF CONTENTS

LIST OF ILLUSTRATIONS

I. INTRODUCTION

The eroding rod model for deep penetration[1,2] is attractive because of its simplicity and its ability to make qualitative predictions that appear to be useful for parametric studies. Nevertheless, it contains several obvious flaws. Chief among these is the use of the modified Bernoulli equation and of the oversimplified rigid/perfectly plastic material model, which is implied by that equation. A critical review of the model as it presently exists is presented in the next section.

In spite of its shortcomings the eroding rod model appears to be a good starting place for an experimental investigation of penetration, which in turn should lead to a more complete model. In the third section of this paper the theoretical framework for an experimental program is described. The theory of one dimensional wave propagation is used to show how data from instrumented long rods and targets may be fitted together to give a coherent picture of the time sequence of events during penetration. Data for one impact condition is then compared within the theoretical framework. In the final section the results to date are discussed.

II. REVIEW OF THE ERODING ROD MODEL

The eroding rod model[1,2] for deep penetration by long rods is based on three simple ideas. First, a long rod penetrator may be considered to be rigid and undeforming, except where it is in contact with the target. There the material erodes and flows at a constant characteristic stress. Second, there is a constant characteristic flow stress in the target. Third, a modified Bernoulli equation holds, which includes the characteristic rod and target stresses. The rod stress, of course, acts to decelerate the intact rear end of the rod. The situation is shown in Fig. 1. The equations expressing these ideas are as follows[2].

$$\text{Balance of Mass:} \qquad \dot{\ell} = \dot{p} - u$$

$$\text{Balance of Momentum:} \qquad \rho_p \, \ell \, \dot{u} = - \Sigma \tag{1}$$

$$\text{Modified Bernoulli:} \qquad \Sigma + \tfrac{1}{2} \rho_p (u-\dot{p})^2 = T + \tfrac{1}{2} \rho_t \, \dot{p}^2$$

$$= \text{stress at rod/target interface}$$

---

[1] *V. P. Alekseevskii, "Penetration of a Rod into a Target at High Velocity," Comb., Expl., and Shock Waves, 2, 99-106 (1966).*

[2] *A. Tate, "A Theory for the Deceleration of Long Rods After Impact," J. Mech. Phys. Solids, 15, 387-399 (1967), and "Further Results in the Theory of Long Rod Penetration," J. Mech. Phys. Solids, 17, 141-150 (1969).*

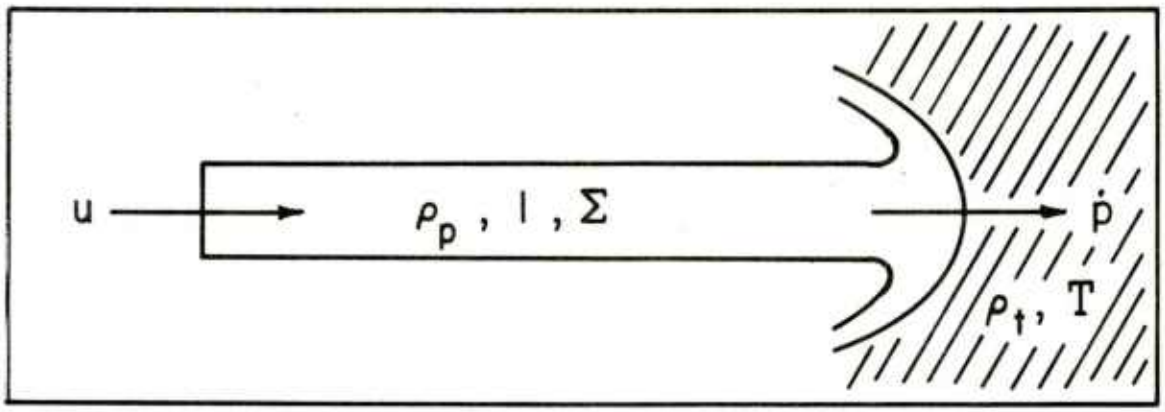

Figure 1. Long Rod Penetrating a Target.

Here ℓ is the instantaneous length of intact rod and u is its instantaneous speed. The depth of penetration is p and the rate of penetration is $\dot{p}$. The densities of rod and target respectively are ρ_p and ρ_t. The characteristic stresses are Σ and T in the rod and target.

Equation $(1)_3$ is solved for $\dot{p}$ and situated in $(1)_1$. This procedure gives three ordinary differential equations for ℓ, p, and u, which are to be solved simultaneously. The integration is not quite straightforward, however, because there are simple physical constraints on $\dot{p}$, namely

$$0 \leq \dot{p} \leq u. \tag{2}$$

The lower limit is required since penetration can only open a hole in the target, never close one. The upper limit is required since it is assumed that penetrator and target are always in contact, but since the penetrator cannot increase in length, $\dot{\ell} \leq 0$ in $(1)_1$.

Now consider the two limiting cases in turn as was done by Tate[2]. When $\dot{p} = 0$, there is no further penetration and no further flow of target material, so the stress in the target must be less than T. If the penetrator is still flowing, then the target stress at the interface from $(1)_3$ is given by

$$\tau = \Sigma + \tfrac{1}{2}\rho_p u^2 \leq T \tag{3}$$

Clearly this can only occur if

$$T > \Sigma$$

and

$$u \leq \left[2(T-\Sigma)/\rho_p\right]^{\frac{1}{2}} \tag{4}$$

Similarly, if $\dot{p} = u$, then $\dot{\ell} = 0$, there is no further flow of rod material, and, therefore, the stress in the rod must be less than Σ. If the target material is still flowing, from $(1)_3$ the rod stress at the interface is given by

$$\sigma = T + \tfrac{1}{2}\rho_t u^2 \leq \Sigma \tag{5}$$

This can only happen if

$$T \leq \Sigma$$

and

$$u \leq \left[2(\Sigma - T)/\rho_t\right]^{\frac{1}{2}} \tag{6}$$

It must be concluded that the material model implicit in the use of the modified Bernoulli equation is the highly idealized case of the rigid/perfectly plastic solid for both penetrator and target as shown in Fig. 2.

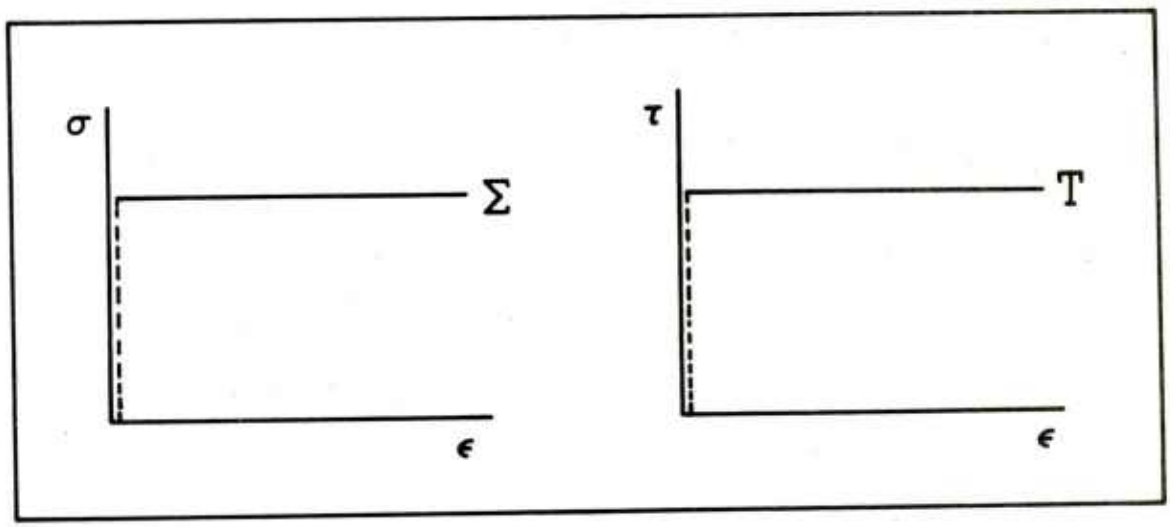

Figure 2. Rigid/Perfectly Plastic Material.

Equations (1) must be replaced by the following set of equations, which satisfy the restrictions outlined above.

$$\dot{\ell} = \dot{p} - u$$

$$\dot{u} = \begin{cases} -(T + \tfrac{1}{2}\rho_t u^2)/\rho_p \ell, & \text{if (6) holds} \\ -\Sigma/\rho_p \ell, & \text{in all other cases} \end{cases}$$

$$\dot{p} = \begin{cases} 0, & \text{if (4) holds} \\ u, & \text{if (6) holds} \\ \dfrac{1}{1-\dfrac{\rho_t}{\rho_p}} \left\{ u - \sqrt{\dfrac{\rho_t}{\rho_p}} \left[u^2 - 2\,\dfrac{\Sigma - T}{\rho_t} \left(1 - \dfrac{\rho_t}{\rho_p}\right) \right]^{\frac{1}{2}} \right\}, \\ \text{in all other cases.} \end{cases} \tag{7}$$

These equations are simple enough to be solved on a programmable hand calculator. Typical integrations of (7) giving depth of penetration as a function of impact speed in non-dimensional form are shown in Fig. 3. The results appear to be qualitatively correct, especially the characteristic S-curve for the case $T>\Sigma$, as shown by the experimental results of Stilp and Hohler[3] and Tate[4]. Equations (7), therefore, have considerable intuitive appeal, combining as they do simplicity with qualitative accuracy, but they are difficult to use quantitatively because values for the characteristic stresses Σ and T are not readily available *a priori*. The usual procedure has been to choose the stresses so as to fit an experimental S-curve, and then to consider them as material constants. Due to the approximations inherent in the model, this procedure is unlikely to be satisfactory. The difficulties are threefold.

The first problem is in the origin of the modified Bernoulli equation itself. In the theory of perfect, incompressible fluids, the Bernoulli equation is obtained in steady flow by integration along a streamline. This gives

$$P + \tfrac{1}{2}\rho v^2 = \text{constant} \tag{8}$$

---

[3] *V. Hohler, and A. J. Stilp, "Penetration of Steel and High Density Rods in Semi-Infinite Steel Targets," Third Int. Symp. Ballistics, Karlsruhe, Germany (1977).*

[4] *A. Tate, K. E. B. Green, P. G. Chamberlain and R. G. Baker, "Model Scale Experiments on Long Rod Penetration," Fourth Int. Symp. Ballistics, Monterey, CA (1978).*

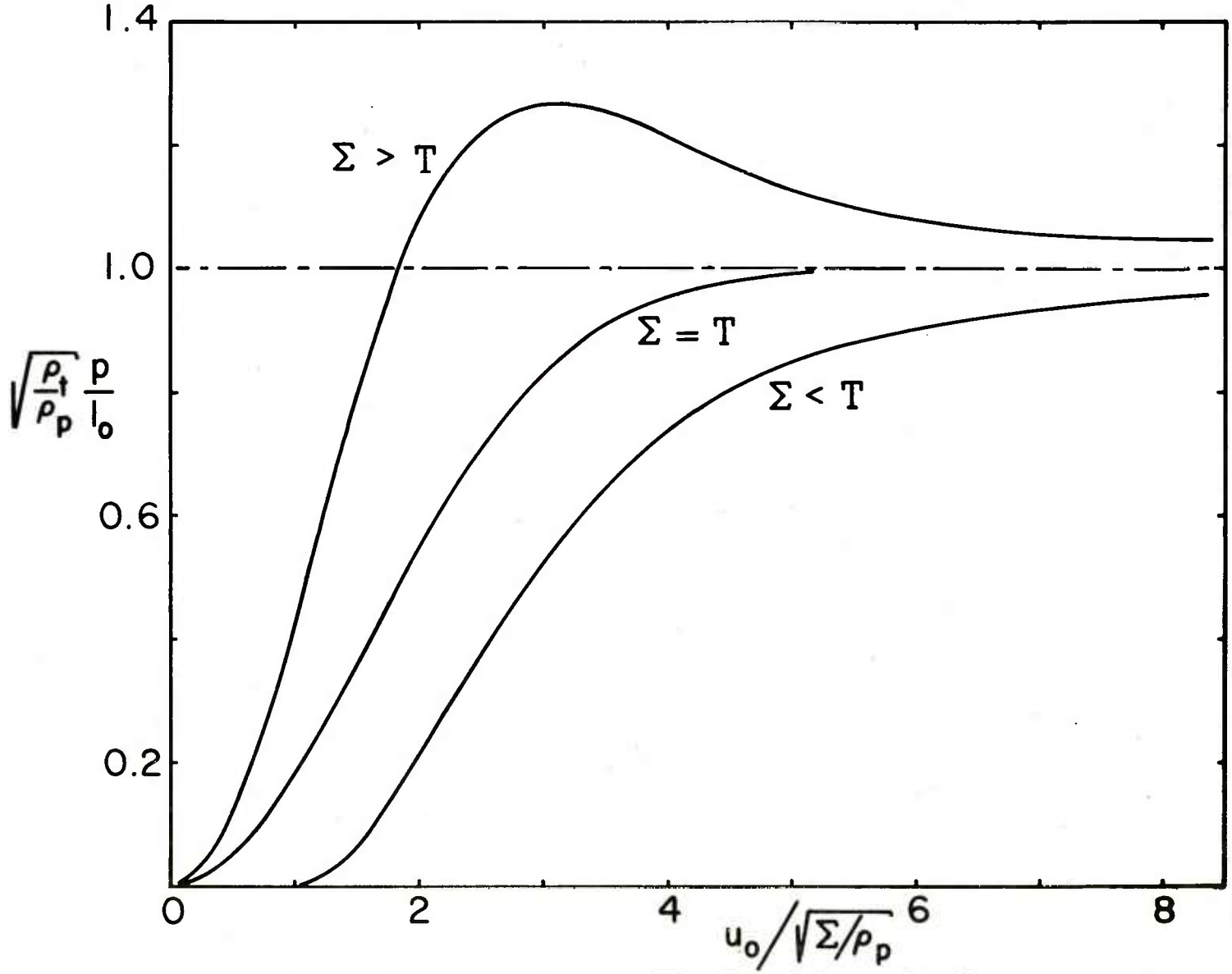

Figure 3. Penetration as a Function of Impact Speed.

where P is pressure. Then by applying the result at a stagnation point and on the stagnation streamline far from the stagnation point in both penetrator and target, and by appealing to the idea of continuity of forces at the stagnation point, the Bernoulli equation as applied to jet interaction is derived[5].

$$\tfrac{1}{2}\,\rho_p\, v^2 = \tfrac{1}{2}\,\rho_t\, w^2 \tag{9}$$

The speeds v and w are measured with respect to the stagnation point.

Now apply the same ideas to the steady motion of a rigid/perfectly plastic solid. With the z-axis and centerline of the rod coinciding in Fig. 1, the z-component of the momentum equation may be written

$$t_{zz,z} + t_{zy,y} + t_{zx,x} = \rho\,(u_{z,t} + u_x u_{z,x} + u_{z,y} + u_z u_{z,})$$

On the centerline $u_x = u_y = 0$ by symmetry, and for steady motion $u_{z,t} = 0$. Shear stresses also vanish on the centerline, but not their derivatives, so integration between points a and b yields

$$t_{zz}(b) - t_{zz}(a) + \int_a^b (t_{zy,y} + t_{zx,x})\, dz \tag{10}$$

$$= \tfrac{1}{2}\,\rho\left[u_z^2(b) - u_z^2(a)\right]$$

Equation (10) is similar to (8) with the important difference of the remaining integral. If equation (10) is to apply to the rod, point b could be fixed in the rod/target interface, and point a could be located at the rigid plastic boundary. The exact location of that boundary is unknown, but within the terms of the material model the stress there must be the constant flow stress, $t_{zz} = -\Sigma$, and the particle speed as it enters the region of steady flow must be the speed of the rigid rear end relative to the interface, $u-\dot{p}$. Similar considerations must apply to the target with the z-component of stress at the rigid/plastic boundary being $t_{zz} = -T$ and the particle speed relative to the interface being $\dot{p}$. Since stress must be continuous at the interface and since the stagnation velocities are zero, the modified Bernoulli equation should read

---

[5]*M. I. Gurevich, Theory of Jets in Ideal Fluids, Academic Press, New York and London (1965).*

$$\Sigma + \tfrac{1}{2}\rho_p(u-\dot{p})^2 + I_p$$

$$= T + \tfrac{1}{2}\rho_t \dot{p}^2 + I_t \qquad (11)$$

$$\text{where } I = \int_a^b (t_{zy,y} + t_{zx,x})\, dz$$

Thus, even within the limitations of the assumptions of a rigid/plastic material and steady flow, the modified Bernoulli equation cannot be strictly true.

The second problem concerns the validity of those assumptions; namely steady flow and a rigid/plastic material. Taken overall, kinetic energy penetration is clearly an unsteady process, especially in the initiation and final stopping or breakout stages, but there may be parts of the process, localized in both space and time, that are nearly steady, as for example, a local interaction region near the penetrator/target interface during the intermediate stages of penetration. In such a domain equation (11) should be valid, but even then there is no clear way to make an accurate estimate of the characteristic stresses. The stress/strain curve of most real materials is not well approximated by the rigid/plastic assumption because of work hardening. For example, a typical curve is shown in Fig. 4. Because the failure processes are

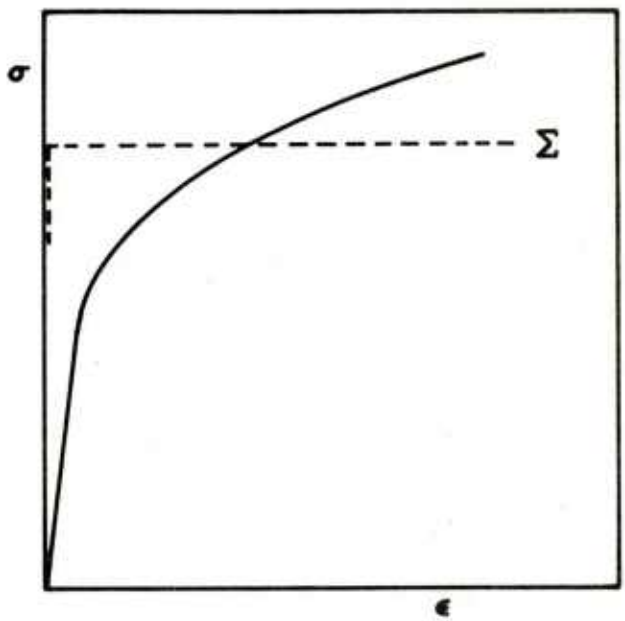

Figure 4. Stress/Strain Curve with Work Hardening and Rigid/Plastic Approximation.

unknown there is no way *a priori* to choose the characteristic or average stress Σ either on the basis of energy equivalence or maximum stress or any other way. In the target the situation is even more muddled. For the rod it has been tacitly assumed that the state of stress is nearly uniaxial, but in the target the stress will be triaxial with a substantial, but unknown spherical component. The matrix of components on the centerline may be represented by

$$\begin{Bmatrix} T_1 & 0 & 0 \\ 0 & T_2 & 0 \\ 0 & 0 & T_3 \end{Bmatrix} = - \begin{Bmatrix} P & 0 & 0 \\ 0 & P & 0 \\ 0 & 0 & P \end{Bmatrix} + \begin{Bmatrix} -S & 0 & 0 \\ 0 & \tfrac{1}{2}S & 0 \\ 0 & 0 & \tfrac{1}{2}S \end{Bmatrix} \tag{12}$$

The first matrix on the right contains the pressure and the second contains the deviatoric components, which are related to the instantaneous flow stress, F, in the usual theory of plasticity[6] by

$$S = \frac{2}{3} F \tag{13}$$

The target resistance stress T is given by

$$T = -T_1 = P + \frac{2}{3} F \tag{14}$$

Because of work hardening and unknown failure processes, the target flow stress is as ill defined as the rod stress, but in addition there is an unknown hydrostatic pressure, which may vary greatly during sequential stages of penetration. A final consequence of real, non-rigid material behavior is that there will be considerable plastic deformation at some distance from the quasi-steady interaction zone. In the rod this has the effect of slowing material down (relative to the rear end) before it reaches that zone so that the speed u to be used in (11) or $(1)_3$ is less than the speed of the rear end. How much less depends on the rate of work hardening. In the target, plastic deformation has the effect of increasing the spatial rate of penetration: that is to say, since real target materials can move ahead of the penetrator, the interface between penetrator and target will move farther in space than it would if the target were rigid in non-plastic regions. Furthermore, inertia will tend to increase the crater size even after the active driving forces have ceased.

The third problem is that the stress tending to decelerate the rod in $(1)_2$ is an average stress over the whole cross section, whereas the stress that enters into the modified Bernoulli equation is the local stress on the centerline. These may be somewhat different from each other.

In summary, then, it has been shown that:

(1) The modified Bernoulli equation cannot hold rigorously because of shear stress gradients in solids;

(2) The deformation processes are steady at most in a limited domain, but even then it is not possible to choose the characteristic stresses Σ and T *a priori* because of work hardening and unknown failure processes. Furthermore, plastic deformation will extend well outside the quasi-steady zone; and

(3) The local centerline stress is unequal to the average cross-sectional stress.

For these reasons the eroding rod model is difficult to use quantitatively and gives only limited insight into the details of the actual rod/target interaction, but in spite of its shortcomings the model appears to contain the germ of a sound theory of penetration, as shown by the qualitative success of its predictions. The model probably averages over the forces and erosion processes in some way so as to achieve partial success.

III. THEORETICAL FRAMEWORK FOR AN EXPERIMENTAL PROGRAM

An experimental program has been devised to begin probing the details of the interaction process. The program is based on the following assumptions and theoretical considerations. Penetration is controlled by flow and failure processes that occur at or near the penetrator/target interface. These processes will depend on the material properties of the particular materials involved, and therefore, they will depend only on the local stress and strain fields. These ideas are at least compatible with the formation of a region of steady flow at the interface. Since it is a local phenomenon, it seems reasonable to suppose that the steady conditions established will depend only on the local geometry and the mass flux through the region. In particular it should not depend at all on the length of the penetrator. This suggests that a long rod with strain gages attached could be used as a probe into the target interior. If the rod is long enough so that wave reflections from the rear cannot interfere with measurements, then the interpretation of the strain data will be considerably simplified. At the same time, any inferences concerning the forces, strains, or particle velocities at the impact end will be equally valid for shorter rods of the same material. In other words, it seems plausible that material characteristics will fix the boundary conditions locally at the impact end. It is the function of the experimental program to determine what those boundary conditions are.

In normal impact the motion of the rod is axi-symmetric. If the rod is treated as a one dimensional continuum where radial motions are ignored, the equations of motion may be written as follows:

$$\sigma_x = \rho u_t$$
$$u_x = \varepsilon_t \tag{15}$$

In (15) σ is the axial stress in the rod (referred to the initial cross-sectional area), ρ is the initial density, u is the particle velocity, and ε is the engineering strain. Subscripts denote partial differentiation where x is the material coordinate in the rod and t is time. The spatial location, x, of a material particle, X, is denoted

$$x = x(X,t) \tag{16}$$

we have

$$u = x_t, \quad \varepsilon = x_X - 1 \tag{17}$$

If strain gages are located at multiple stations along the rod in an impact experiment, then strain as a function of time can be recorded at each station, and by interpolation strain will also be known at all other stations as well. Instrumented rod experiments of this type have been conducted by Hauver over the past several years. He uses a light-gas gun where an evacuated target chamber and accurate alignment permit data of unusually high quality to be obtained. Complete experimental details are reported by him in other papers[7,8], but the experimental conditions, in brief, were as follows. A long steel rod, (S-7 tool steel, hardened to RC47), with length of 254mm and diameter of 8.13mm, impacts at normal incidence against a 25.4mm plate of rolled homogeneous armor at RC27. Speed of impact was nominally 1000 m/s for most tests, and 710 m/s in a few others. Strain was measured in the rod as a function of time, usually at stations 20, 40, 60, and 80mm from the impact end.

With ε-t data at hand, curves of constant strain may be plotted in X-t space. Along such a curve the slope, defined as c_p, the plastic wave speed, may be measured and related to derivatives of strain as follows.

---

[7] *G. E. Hauver, "Penetration with Instrumented Rods," Int. J. Eng. Sci., 16, 871-877 (1978).*

[8] *G. E. Hauver, "Experiments with Instrumented Long-Rod Penetrators," Fifth Int. Symp. Ballistics, Toulouse, France (1980).*

$$d\varepsilon = \varepsilon_t\, dt + \varepsilon_x dX = 0$$
$$\frac{dX}{dt} = c_p = -\frac{\varepsilon_t}{\varepsilon_x} \tag{18}$$

These curves need not be straight lines, but if they are, as all experiments to date indicate, the analysis is greatly simplified because c_p then depends only on ε. Equations (15) may be integrated with respect to X along lines t = constant as was described by Kolsky[9] and others. If the rod has speed u_o and zero stress and strain at any station before a wave arrives, we have

$$u(X,t) = u_o + \int_{\infty}^{X} \varepsilon_t(X,t)\, dX$$
$$= u_o - \int_{o}^{\varepsilon(X,t)} c_p(\varepsilon)\, d\varepsilon \tag{19}$$

$$\sigma(X,t) = \int_{\infty}^{X} \rho\, u_t(X,t)\, dX$$
$$= \int_{o}^{\varepsilon(X,t)} \rho c_p^2(\varepsilon)\, d\varepsilon \tag{20}$$

Note that the stress has been obtained in (20) without recourse to any constitutive assumption. In fact, a dynamic stress-strain relation has been computed from the experimental data using only the simple one dimensional equations of motion and compatibility.

Equations (19) and (20) determine the particle velocity and stress everywhere in the rod in principle. Thus, if the rate of rod erosion were known, these quantities would be known for the rod as it enters the quasi-steady region near the penetrator/target interface. The situation is shown in Fig. 5. The rays of constant strain are taken from Ref. 8.

The timing of gage failure cannot be used to establish the unknown erosion trajectory because gages are typically destroyed by ejecta before reaching the interface[8]. Independent experiments by Netherwood have measured the rate of penetration into the target directly[10] for the same materials and impact conditions as in Hauver's experiments. Complete details are given in his paper, but essentially his technique was to

---

[9] *H. Kolsky, Stress Waves in Solids, Dover Publications, New York (1963).*

[10] *P. H. Netherwood, "Rate of Penetration Measurements," ARBRL-MR-02978, Ballistic Research Laboratory, Aberdeen Proving Ground, MD, Dec. 1979.*

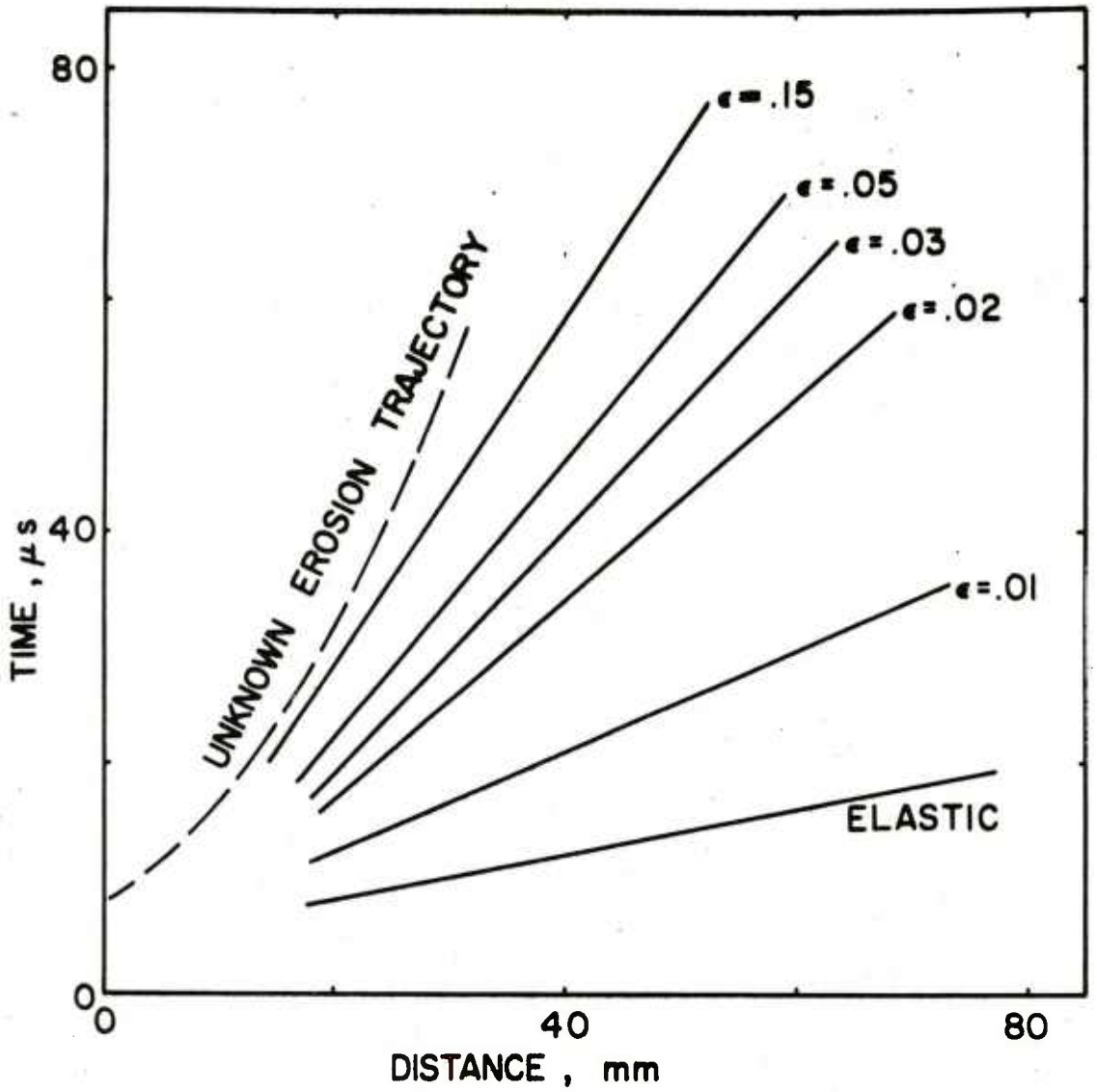

Figure 5. Lines of Constant Strain in X-t Space with Unknown Erosion Trajectory [after Hauver[8]].

insert contact switches into the target block through holes drilled from the side. The timing of switch triggering then gives the trajectory of the penetrator/target interface in target material coordinates. Fig. 6 shows a compilation of data obtained by Netherwood[10]. The unsteady entry region is clearly shown, followed by a steady intermediate region and an erratic, final, unsteady region.

The final apparent increase in speed is probably due to pins shearing ahead of the penetrator as a small plug forms. The penetration trajectory may be compared with strain data, measured in material coordinate in the rod, if both sets of data can be transformed into a common coordinate system.

Fortunately, all data may be easily transformed, at least approximately, into laboratory coordinates. For the penetration data the transformation is a simple, time dependent translation. As penetration progresses the rear surface of the target bulges and finally fails by plugging. Netherwood has measured this motion of the rear surface with a streak camera[11]. If deformation between switch pin and rear surface is neglected, then the translation of the pin in front of the penetrator is the same as that of the rear target surface. Target deformation remains completely unknown, but would contribute only a small correction compared to overall translation.

Rod data can also be transformed into laboratory coordinates. Since particle velocity is known as a function of position and time from (19), integration with respect to time will give trajectories in laboratory coordinates for each rod station. Hauver has computed some of these trajectories[8]. It turns out to be more instructive to plot spatial trajectories of constant strain. From (16), with $X = X(t)$ being a curve of constant strain in material coordinates, differentiation yields the following equation.

$$\frac{dx}{dt} = \frac{\partial x}{\partial t} + \frac{\partial x}{\partial X}\frac{dX}{dt}$$

With the aid of (17), (18), and (19) this becomes

$$\frac{dx}{dt} = u_o - \int_o^{\varepsilon} c_p \, d\varepsilon + (1+\varepsilon)c_p \qquad (21)$$

Several of these curves are plotted in Fig. 7. Both X and x are positive to the right, and u_o is positive, but both c_p and ε are negative since strains are compressive, and plastic waves progress to the left into the rod. Note that curves of constant strain are straight lines in

---

[11] *P. H. Netherwood, private communication.*

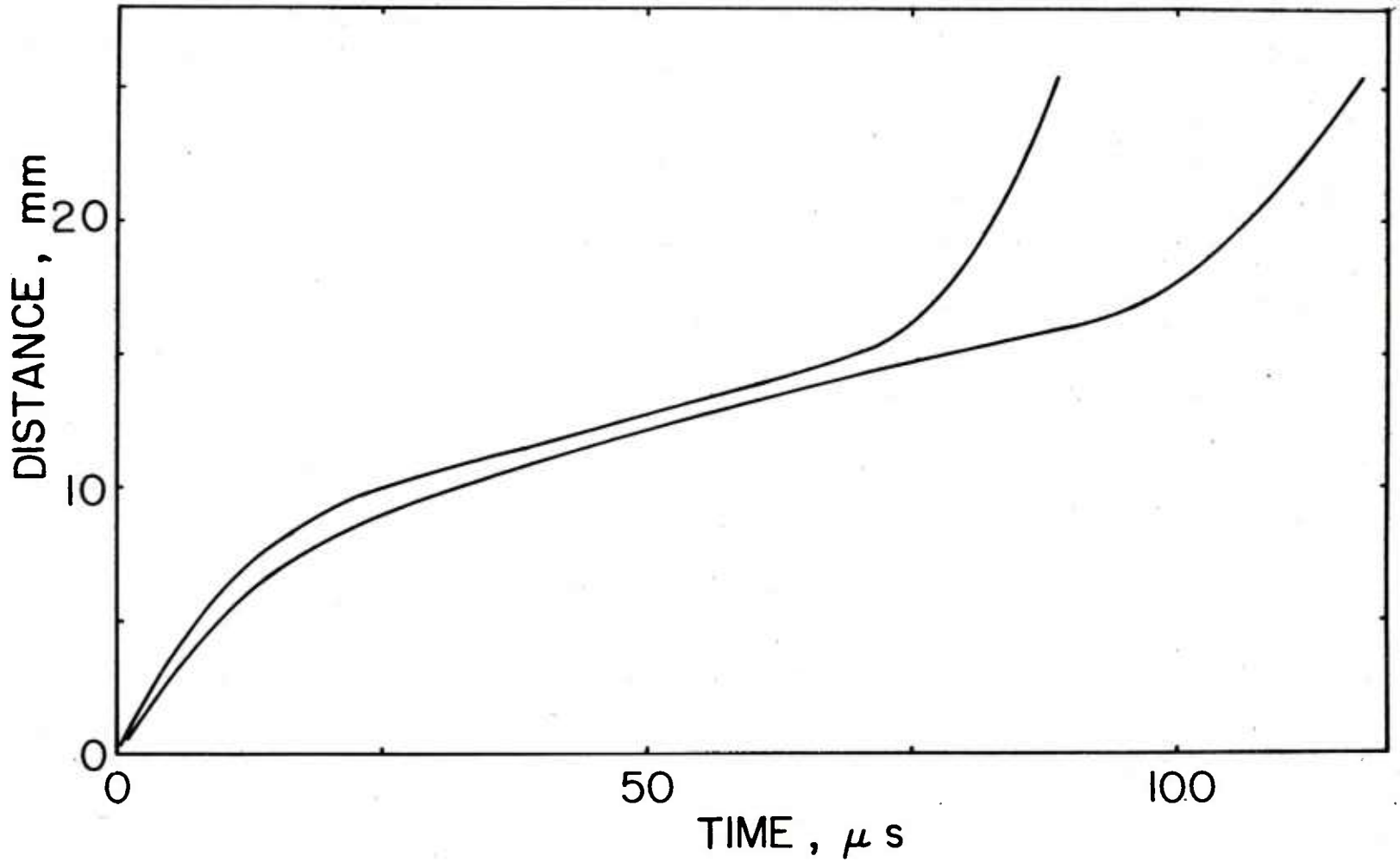

Figure 6. Envelopes of all Data Showing Penetration vs. Time in Target Coordinates from Ref. 10.

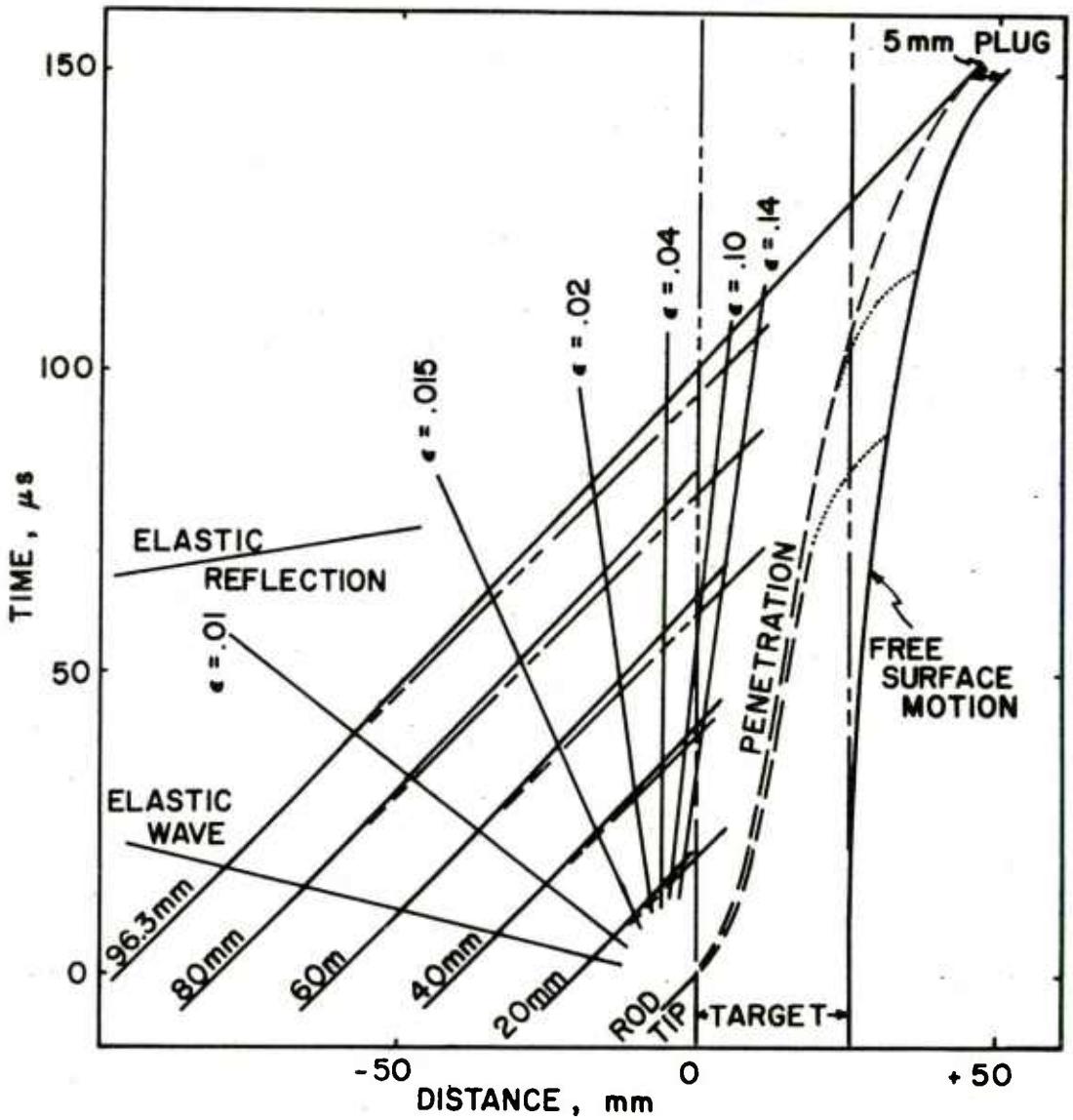

Figure 7. Trajectories in Laboratory Coordinates of Rod Stations, Penetration, Target Free Surface, and Curves of Constant Strain.

x-t space if they are straight in X-t space. Also shown in Fig. 7 is the back surface motion from Ref. 11 and the translated penetration trajectory. In some of his experiments Netherwood recovered the residual penetrator, whose initial, undeformed length was determined by weighing, and a small plug approximately 5mm thick. The trajectories of the leading station of the residual penetrator, labeled 96.3mm, and of the final plug are also shown.

IV. DISCUSSION OF RESULTS

Figures 6 and 7 contain a great deal of useful, albeit incomplete, information about the penetration process. In Fig. 6 the unsteady entry region seems to be about one penetrator diameter in width. The intermediate region shows a nearly constant speed of penetration, which is consistent with the idea of a zone of steady state deformation in penetrator and target.

There is no way of determining whether or not a switch triggers slightly before penetrator arrival in material coordinates, but since it could not be late, the measured arrival times are lower bounds. In any case, in the steady central section of penetration, it seems reasonable to assume that each switch is early by the same amount, on average, so that the true curve would be parallel to the one drawn in its middle section with corresponding minor adjustments in the unsteady end sections. The width of the breakout zone, about 9mm, is also approximately one penetrator diameter, although it is suspicious that one switch pin was usually located at the beginning of that zone and may have played a role in its initiation. Since the recovered plug was only about 5mm thick rather than 9mm, it seems clear that erosion of penetrator and target continues during plug formation and acceleration.

In Fig. 7 curves of constant strain, the penetration curve, back surface motion, and trajectories of selected rod stations are all shown in laboratory coordinates. There is actually considerable extrapolation of data here since strain gage records end near the target surface due to interference from ejecta[8], and the penetration curve ends at the start of plug formation. The free surface data do extend to 150μs, however, and serve to anchor the trajectory extrapolations for penetration and for the 96.3mm station. These three curves (i.e., free surface, penetration, and 96.3mm station) together with the known plug thickness give a remarkably coherent picture.

Strains higher than 14% were measured at one or two stations, but determination of c_p becomes unreliable so that trajectories for higher strains are not shown. Nevertheless, the figure clearly suggests that the leading edge of the fan of constant strains might be roughly parallel to the penetration trajectory. If this were true, then equation (21) would give an estimate of rate of penetration possible for various levels of maximum strain. At the very least it will give a lower bound estimate

for $\dot{p}$. This bound as a function of strain is plotted in Fig. 8 for the case considered. The measured value for $\dot{p}$, taken from Fig. 7, is about 190 m/s, which is not much greater than the maximum of the lower bound. Note that the bound, as given by equation (21), is linear in the impact speed u_o so that other cases may be considered simply by moving the horizontal axis up or down, provided the shape of the curve does not change too much with u_o.

Successful measurements have now been made of Σ, u, and $\dot{p}$ in equation (11). Another series of experiments to measure T directly for the same impact conditions are also under way by Pritchard at BRL. This leaves only the two terms I_p and I_t, which cannot be measured directly, but perhaps could be estimated analytically.

In future experimental work, the speed of impact, target thickness, and penetrator material will be varied. At the same time the analysis is being extended to include the effects of radial motion of rod material since the assumption of one-dimensional motion in equation (15) is probably not completely adequate.

The investigation of detailed interactions during penetration has been guided by a theoretical framework that is based on the one dimensional theory of wave propagation. Although this work has not yet led to a replacement for the eroding rod model, it has led to an experimental description of events against which any successor model may be evaluated.

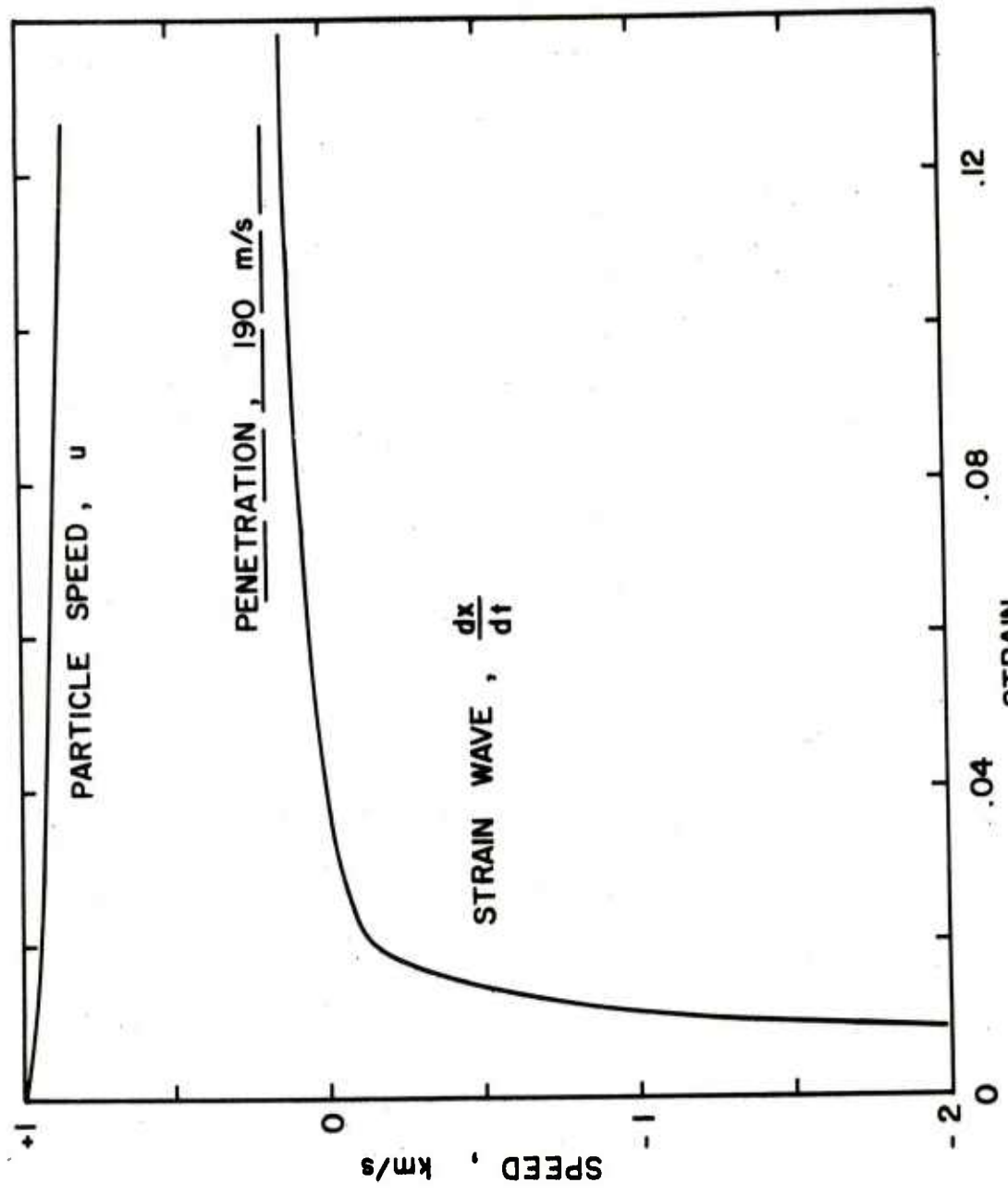

Figure 8. Particle Speed, u, and Speed of Strain Wave, dx/dt, vs. Strain, ε.

REFERENCES

1. V. P. Alekseevskii, "Penetration of a Rod into a Target at High Velocity," Comb., Expl., and Shock Waves, 2, 99-106 (1966).

2. A. Tate, "A Theory for the Deceleration of Long Rods After Impact," J. Mech. Phys. Solids, 15, 387-399 (1967), and "Further Results in the Theory of Long Rod Penetration," J. Mech. Phys. Solids, 17, 141-150 (1969).

3. V. Hohler, and A. J. Stilp, "Penetration of Steel and High Density Rods in Semi-Infinite Steel Targets," Third Int. Symp. Ballistics, Karlsruhe, Germany (1977).

4. A. Tate, K. E. B. Green, P. G. Chamberlain and R. G. Baker, "Model Scale Experiments on Long Rod Penetration," Fourth Int. Symp. Ballistics, Monterey, CA (1978).

5. M. I. Gurevich, Theory of Jets in Ideal Fluids, Academic Press, New York and London (1965).

6. R. Hill, The Mathematical Theory of Plasticity, Oxford University Press, London (1950).

7. G. E. Hauver, "Penetration with Instrumented Rods," Int. J. Eng. Sci., 16, 871-877 (1978).

8. G. E. Hauver, "Experiments with Instrumented Long-Rod Penetrators," Fifth Int. Symp. Ballistics, Toulouse, France (1980).

9. H. Kolsky, Stress Waves in Solids, Dover Publications, New York (1963).

10. P. H. Netherwood, "Rate of Penetration Measurements," ARBRL-MR-02978, Ballistic Research Laboratory, Aberdeen Proving Ground, MD, Dec. 1979.

11. P. H. Netherwood, private communication.

DISTRIBUTION LIST

No. of Copies	Organization
12	Commander Defense Technical Info Center ATTN: DDC-DDA Cameron Station Alexandria, VA 22314
1	Deputy Assistant Secretary of the Army (R&D) Department of the Army Washington, DC 20310
1	HQDA (DAMA-ARP-P, Dr. Watson) Washington, DC 20310
1	HQDA (DAMA-MS) Washington, DC 20310
1	Commander US Army Ballistic Missile Defense Systems Command ATTN: SENSC, Mr. Davidson P. O. Box 1500 Huntsville, AL 35804
1	Director US Army Ballistic Missile Defense Systems Office 1320 Wilson Boulevard Arlington, VA 22209
1	Director US Army Advanced BMD Technology Center ATTN: CRDABH-5, W. Loomis P.O. Box 1500, West Station Huntsville, AL 35807
1	Commander US Army War College ATTN: Lib Carlisle Barracks, PA 17013
1	Commander US Army Command and General Staff College ATTN: Archives Fort Leavenworth, KS 66027
1	Commander US Army Materiel Development and Readiness Command ATTN: DRCDMD-ST 5001 Eisenhower Avenue Alexandria, VA 22333
4	Commander US Army Armament Research and Development Command ATTN: DRDAR-TSS (2 cys) DRDAR-SC, Dr. E. Bloore DRDAR-LC, Dr. J. Frasier Dover, NJ 07801
1	Commander US Army Armament Materiel Readiness Command ATTN: DRSAR-LEP-L, Tech Lib Rock Island, IL 61299
3	Director US Army Armament Research and Development Command Benet Weapons Laboratory ATTN: DRDAR-LCB-TL Dr. F. Schneider Dr. T. Davidson Watervliet, NY 12189
1	Commander US Army Aviation Research and Development Command ATTN: DRSAV-E P. O. Box 209 St. Louis, MO 63166

DISTRIBUTION LIST

No. of Copies	Organization
1	Director US Army Air Mobility Research and Development Laboratory Ames Research Center Moffett Field, CA 94035
1	Commander US Army Communications Rsch and Development Command ATTN: DRDCO-PPA-SA Fort Monmouth, NJ 07703
1	Commander US Army Electronics Research and Development Command Technical Support Activity ATTN: DELSD-L Fort Monmouth, NJ 07703
1	Commander US Army Harry Diamond Labs ATTN: DELHD-TA-L 2800 Powder Mill Road Adelphi, MD 20783
1	Commander US Army Missile Command ATTN: DRSMI-R Redstone Arsenal, AL 35809
1	Commander US Army Missile Command ATTN: DRSMI-YDL Redstone Arsenal, AL 35809
2	Commander US Army Mobility Equipment Research & Development Cmd ATTN: DRDME-WC DRSME-RZT Fort Belvoir, VA 22060
1	Commander US Army Natick Research and Development Center ATTN: DRXRE, Dr. D. Sieling Natick, MA 01762
1	Commander US Army Tank Automotive Research & Development Cmd ATTN: DRDTA-UL Warren, MI 48090
1	Commander US Army Electronics Proving Ground ATTN: Tech Lib Fort Huachuca, AZ 85613
3	Commander US Army Materials and Mechanics Research Center ATTN: DRXMR-T, J. Mescall R. Shea S. C. Chou Watertown, MA 02172
3	Commander US Army Research Office ATTN: Dr. G. Mayer Dr. F. Schmiedeshoff Dr. E. Saibel P. O. Box 12211 Research Triangle Park NC 27709
1	Director US Army TRADOC Systems Analysis Activity ATTN: ATAA-SL, Tech Lib White Sands Missile Range NM 88002

DISTRIBUTION LIST

No. of Copies	Organization
1	Office of Naval Research Department of the Navy ATTN: Code 402 Washington, DC 20360
1	Commander Naval Surface Weapons Center ATTN: Code GR-9, Dr. W.Soper Dahlgren, VA 22448
1	Commander Naval Weapons Center ATTN: Code 3813, M.Backman China Lake, CA 93557
1	Commander and Director Naval Electronics Laboratory ATTN: Lib San Diego, CA 92152
4	Commander Naval Research Laboratory ATTN: Code 5270, F.MacDonald Code 2020, Tech Lib Code 7786, J. Baker C. Sanday Washington, DC 20375
1	Commanding General Fleet Marine Force, Atlantic ATTN: G-4 (NSAP) Norfolk, VA 23511
1	AFATL (DLDG) Eglin AFB, FL 32542
1	AFATL (DLDL, MAJ J. D. Morgan) Eglin AFB, FL 32542
1	AFATL (DLYW) Eglin AFB, FL 32542
1	AFATL (J. Smith) Eglin AFB, FL 32542
1	RADC (EMTLD, Lib) Griffiss AFB, NY 13440
1	AUL (3T-AUL-60-118) Maxwell AFB, AL 36112
1	AFFDL/FB (Dr. J. Halpin) Wright-Patterson AFB, OH 45433
1	AFML (Dr. T. Nicholas) Wright-Patterson AFB, OH 45433
1	Director Lawrence Livermore Laboratory ATTN: Dr. M. Wilkins Livermore, CA 94550
4	Sandia National Laboratories ATTN: Dr. L. Davison Dr. P. Chen Dr. L. Bertholf Dr. W. Herrmann Albuquerque, NM 87115
1	IBM Watson Research Center ATTN: R.A. Toupin Poughkeepsie, NY 12601
5	Brown University Division of Engineering ATTN: Prof. R. Clifton Prof. H. Kolsky Prof. A. Pipkin Prof. P. Symonds Prof. J. Martin Providence, RI 02192
3	California Institute of Tech Division of Engineering and Applied Science ATTN: Dr. J. Miklowitz Dr. E. Sternberg Dr. J. Knowles Pasadena, CA 91102

DISTRIBUTION LIST

No. of Copies	Organization
4	Carnegie Mellon University Department of Mathematics ATTN: Dr. D. Owen Dr. M. E. Gurtin Dr. B. Coleman Dr. W. Williams Pittsburgh, PA 15213
2	Catholic University of America School of Engineering and Architecture ATTN: Prof. A. Durelli Prof. J. McCoy Washington, DC 20017
1	Harvard University Division of Engineering and Applied Physics ATTN: Dr. G. Carrier Cambridge, MA 02138
2	Iowa State University Engineering Research Lab ATTN: Dr. G. Nariboli Dr. A. Sedov Ames, IA 50010
4	Johns Hopkins University ATTN: Prof. J. Bell Prof. R. E. Green Prof. C. A. Truesdell Prof. J. L. Ericksen 34th and Charles Streets Baltimore, MD 21218
2	Lehigh University Center for the Application of Mathematics ATTN: Dr. E. Varley Dr. R. Rivlin Bethlehem, PA 18015
1	Massachusetts Institute of Technology ATTN: Dr. R. Probstein 77 Massachusetts Avenue Cambridge, MA 02139
1	New York University Department of Mathematics ATTN: Dr. J. Keller University Heights New York, NY 10053
2	North Carolina State University Department of Engineering Mechanics ATTN: Dr. W. Bingham Dr. Y. Horie P. O. Box 5071 Raleigh, NC 27607
1	Pennsylvania State University Engineering Mechanical Dept. ATTN: Prof. N. Davids University Park, PA 16502
1	Forrestal Research Center Aeronautical Engineering Lab Princeton University ATTN: Dr. A. Eringen Princeton, NJ 08540
1	Purdue University Institute for Mathematical Sciences ATTN: Dr. E. Cumberbatch Lafayette, IN 47907
2	Rice University ATTN: Dr. R. Bowen Dr. C. C. Wang P. O. Box 1892 Houston, TX 77001

DISTRIBUTION LIST

No. of Copies	Organization
1	Southern Methodist University Solid Mechanics Division ATTN: Prof. H. Watson Dallas, TX 75221
2	Southwest Research Institute Department of Mechanical Sciences ATTN: Dr. U. Lindholm Dr. W. Baker 8500 Culebra Road San Antonio, TX 78228
3	SRI International ATTN: D. Curran L. Seaman Y. Gupta Menlo Park, CA 94025
1	Temple University College of Engineering Tech. ATTN: Dr. R. M. Haythornthwaite, Dean Philadelphia, PA 19122
1	Tulane University Dept of Mechanical Engineering ATTN: Dr. S. Cowin New Orleans, LA 70112
2	University of California ATTN: Dr. M. Carroll Dr. W. Goldsmith Berkleley, CA 94704
1	University of California Dept. of Aerospace and Mechanical Engineering Science ATTN: Dr. Y. C. Fung P. O. Box 109 La Jolla, CA 92037
1	University of California Department of Mechanics ATTN: Dr. R. Stern 504 Hilgard Avenue Los Angeles, CA 90024
1	University of Delaware Department of Mechanical Engineering ATTN: Prof. J. Vinson Newark, DE 19711
2	University of Houston Department of Mechanical Engineering ATTN: Dr. T. Wheeler Dr. R. Nachlinger Houston, TX 77004
1	University of Illinois Dept. of Theoretical and Applied Mechanics ATTN: Dr. D. Carlson Urbana, IL 61801
2	University of Illinois at Chicago Circle College of Engineering Dept. of Materials Engineering ATTN: Prof. A. Schultz Dr. T. C. T. Ting P. O. Box 4348 Chicago, IL 60680
1	University of Iowa ATTN: Dr. L. Valanis Iowa City, IA 52240

DISTRIBUTION LIST

No. of Copies	Organization
4	University of Kentucky Dept. of Engineering Mechanics ATTN: Dr. M. Beatty Prof. O. Dillon, Jr. Prof. P. Gillis Dr. D. Leigh Lexington, KY 40506
2	The University of Maryland Department of Mechanical Engineering ATTN: Prof. J. Yang Dr. J. Dally College Park, MD 20742
1	University of Minnesota Dept. of Engineering Mechanics ATTN: Dr. R. Fosdick Minneapolis, MN 55455
1	University of Notre Dame Department of Metallurgical Engineering and Materials Sciences ATTN: Dr. N. Fiore Notre Dame, IN 46556
1	University of Pennsylvania Towne School of Civil and Mechanical Engineering ATTN: Prof. Z. Hashin Philadelphia, PA 19105
4	University of Texas Department of Engineering Mechanics ATTN: Dr. M. Stern Dr. M. Bedford Prof. Ripperger Dr. J. T. Oden Austin, TX 78712
1	University of Washington Department of Mechanical Engineering ATTN: Prof. J. Chalupnik Seattle, WA 98105
2	Yale University ATTN: Dr. B. Chu Dr. E. Onat 400 Temple Street New Haven, CT 96520
2	Washington State University Department of Physics ATTN: Dr. R. Fowles Dr. G. Duvall Pullman, WA 99163

Aberdeen Proving Ground

Dir, USAMSAA
ATTN: DRXSY-MP, H. Cohen
Cdr, USATECOM
ATTN: DRSTE-TO-F
Dir, USACSL
Bldg. E3516, EA
ATTN: DRDAR-CLB-PA